Fluxes of gaseous elemental mercury (GEM) in the High Arctic during atmospheric mercury depletion events (AMDEs)

Jesper Kamp[1,2], Henrik Skov[1,3], Bjarne Jensen[1,3] and Lise Lotte Sørensen[1,3]

[1]Arctic Research Centre, Aarhus University, 8000 Aarhus, Denmark
5 [2]Department of Engineering, Aarhus University, 8000 Aarhus, Denmark
[3]Department of Environmental Science, Aarhus University, 4000 Roskilde, Denmark

Correspondence to: Henrik Skov (HSK@envs.au.dk)

Abstract. Measurements of gaseous elemental mercury (GEM) fluxes over snow surfaces using a relaxed eddy accumulation
10 (REA) system are carried out at the High Arctic site Villum Research Station, Station Nord in North Greenland.
Simultaneously, CO_2 fluxes are determined using the eddy covariance (EC) technique. The REA system with a dual-inlets
and dual-analyzers are used to measure fluxes directly over the snow. The measurements were carried out from April 23 to
May 12 during spring 2016, where atmospheric mercury depletion events (AMDEs) took place. The measurements showed a
net emission of 8.9 ng m^{-2} min^{-1}, with only a few depositional fluxes, a maximum deposition of 8.0 ng m^{-2} min^{-1} and a
15 maximum emission of 190 ng m^{-2} min^{-1}. The data support the theory that gaseous oxidized mercury (GOM) is deposited
during AMDEs followed by formation of GEM on surface snow and is reemitted as GEM shortly after the AMDEs. The
measurements also indicate GEM emission is increasing with increasing temperature, supporting that surface heating
controls GOM reduction in the surface layer of the snow.

1 Introduction

20 Mercury (Hg) is a toxic element found in the atmosphere primarily as elemental mercury. Airborne Hg can have several
forms: gaseous oxidized mercury (GOM), particulate bound mercury (PBM) or gaseous elemental mercury (GEM). PBM
and GOM are removed faster from the atmosphere than GEM and have atmospheric lifetimes on the order of days (Sørensen
et al., 2010;Goodsite et al., 2004, 2012;Valente et al., 2007). Thus, GOM and PBM generally deposit near emission sources.
The lifetime of GEM is determined by the reaction between GEM and Br (Goodsite et al., 2012, 2004), and spans from one
25 to two months (Holmes et al., 2006;Sørensen et al., 2010). Thus, GEM can be transported over longer distances to areas with
low natural and anthropogenic emissions. GEM concentrations in the Arctic are mainly due to long-range transportation
from lower latitude sources (Dastoor et al., 2008;Pandey et al., 2011;Christensen et al., 2004). However, in the Arctic, during
polar spring, the lifetime of GEM can be as short as roughly 10 hours (Berg et al., 2013;Steffen et al., 2008;Skov et al.,
2004). Furthermore, the oxidation chemistry of Hg^0 is still inexplicit and the relaxation time of mercury in the atmosphere

could be longer due to reduction of Hg^{II} in cloud droplets and/or in the sea, e.g. Angot et al. (2016) and Travnikov et al. (2017).

In the Arctic, sub-Arctic and Antarctic rapid decrease in GEM concentration in coastal areas has been observed during spring (Ebinghaus et al., 2002;Berg et al., 2013;Skov et al., 2004;Schroeder et al., 1998;Steffen et al., 2008). These

5 atmospheric mercury depletion events (AMDEs) cause significant Hg deposition in Polar Regions (Steffen et al., 2008;Dastoor et al., 2008). During AMDEs, GEM is depleted from the atmosphere by oxidation to GOM (Skov et al., 2004;Toyota et al., 2014), which is then deposited locally due to fast deposition limited only by aerodynamic resistance (Skov et al., 2006). Mercury bio-accumulates in Arctic marine wildlife through the food web. Thus, this is a human health concern in Arctic communities due to high mercury exposure through the traditional indigenous diet (AMAP, 2011).

10 Typical Arctic spring conditions such as low temperatures, sunlight and reactive halogens favor AMDEs (Brooks et al., 2006;Steffen et al., 2015;Goodsite et al., 2004, 2012;Berg et al., 2003). In earlier studies (Skov et al., 2004;Schroeder et al., 1998), depletion of ozone during AMDEs revealed a correlation between ozone and GEM concentration. Ozone concentration decreases during reaction with bromine: $O_3 + Br \rightarrow O_2 + BrO$ (Hausmann and Platt, 1994). Data from Villum Research Station (VRS), Station Nord in North Greenland suggests a mutual reactant responsible for the removal of GEM

15 and ozone that agreed with Br reactions during AMDEs (Skov et al., 2004).

Following AMDEs, elevated concentrations of GEM have been observed (Lalonde et al., 2002;Steffen et al., 2008), and it is suggested that photochemical processes in the snow reduce deposited Hg back to GEM, which is then reemitted into the atmosphere (Ferrari et al., 2004;Lalonde et al., 2002). Vertical gradient measurements and measurements from interstitial air in snow indicate GEM emission at the snow surface (Ferrari et al., 2004;Steffen et al., 2002). The reduction to GEM is

20 assumed to take place in the aqueous phase and potentially in particles with significant water content (Steffen et al., 2015).

Knowledge of the dynamics of Hg in snow during AMDEs is important in order to understand the fate of GEM. Studies of Hg in snow evince an increase from February and peak in May (Steffen et al., 2014). This is likely due to the accumulation of deposited GOM, and this finding corresponds well with the peak occurrence of AMDEs in April and May (Steffen et al., 2015). A number of specific conditions and parameters, such as temperature, radiation and chemical composition of the

25 snow affects the dynamics of Hg in the snowpack (Lalonde et al., 2002), but Hg in snow is mainly found in oxidized forms (Steffen et al., 2008).

The dynamics of Hg in snowpack have been studied previously, e.g. by Faïn et al. (2013) who observed complex GEM variations at a mid-latitude site in Colorado, USA. They found that GEM concentration in the top layers of the snowpack increased with increasing solar radiation, suggesting GEM production in the snowpack (Faïn et al., 2013) and that GEM

30 production follows AMDE (Brooks et al., 2006). Thus, it is likely that a correlation between solar radiation-induced parameters such as heat flux or temperature change and GEM production and GEM fluxes exists, making it relevant to look into temperature, radiation and heat flux in relation to GEM flux.

A recent non-Arctic study with a similar setup to measure GEM flux during snowmelt in Degerö, Sweden revealed diurnal variations of fluxes showing deposition from midnight to noon and emissions from noon to midnight with a mean of 3.0±3.8

ng m^{-2} h^{-1} (Osterwalder et al., 2016). Furthermore, Osterwalder et al. (2016) found significant difference between GEM fluxes during unstable, stable, and neutral conditions with a near-zero flux during stable conditions, emission during unstable conditions and deposition during neutral conditions.

Previous GEM flux studies in the Arctic were mainly performed using chamber methods (e.g. Ferrari et al. (2008)) and the
5 aerodynamic gradient method (AGM) (e.g. (Brooks et al., 2006;Cobbett et al., 2007)). The overview in Table 1 clearly shows the large variations in GEM fluxes found by studies in the Arctic.

The aim of the study presented here is to enhance the understanding of the processes controlling the fluxes of GEM over snow-covered surfaces during the Arctic spring, where AMDEs take place. The relaxed eddy accumulation (REA) method (Businger and Oncley, 1990) is used for the flux measurement in a setup with a dual inlet (Cobos et al., 2002;Osterwalder et
10 al., 2016) and dual detectors. GEM fluxes have been determined with REA previously over agricultural soil (Cobos et al., 2002), in a winter wheat cropland (Sommar et al., 2013;Zhu et al., 2015a), in an urban environment, and in boreal peatland (Osterwalder et al., 2016), but never in the Arctic.

2 Materials and methods

2.1 Measurement site

15 From April 23 to May 12 of 2016, measurements of GEM flux, CO_2 flux, GEM concentration, wind speed, wind direction, atmospheric stability and temperature were carried out at "Flyger's hut", a part of Villum Research Station, Station Nord (VRS). The hut is located 2.5 km southeast of the central complex of the Danish military base Station Nord in North Greenland (81˚36' N, 16˚40' W) (Figure 1). The station is located in the world's largest national park (Rasch et al., 2015). Flyger's hut is located at 81˚34.90' N, 16˚37.19' W southeast of Station Nord to minimize influence from local air pollution.
20 The hut has been used as a monitoring site for the Arctic Monitoring and Assessment Programme (AMAP, 2011), since 1994. At this latitude, the polar day lasts from mid-April to September and the polar night lasts from mid-October until the end of February. The dominant wind directions measured locally are from the southwest, potentially with katabatic winds from the Greenlandic ice cap southwest of Flyger's hut. The wind distribution during the campaign is shown in Figure 2.

At the beginning of the measuring period at the end of April, the snow depth was 1.02-1.03 m. Little precipitation was
25 observed and the snow depth varied between 0.94 m and 1.09 m during the campaign. When we ended the measurements, the depth was 1.00-1.03 m. The changes in snow depth are due to blowing snow or sublimation as the temperature never rose above -1.7˚C, with a mean temperature of -16.7˚C. Snowmelt did not remove the snow until mid-July.

2.2 Air mass trajectories

To evaluate the origin of the air masses, backwards trajectories were calculated using the NOAA HYSPLIT model (Rolph et
30 al., 2017;Stein et al., 2015). Trajectories are calculated every six hours as 24-hour backwards trajectories from a starting

point at VRS at 20 meter above ground level. Four examples of trajectory plots of single trajectories and trajectory frequency
are shown in Figures 3 and 4.

2.3 Local meteorological measurements

An ultrasonic anemometer (METEK, uSonic-3 Scientific), installed at 6.40 m above ground level, was used to measure the
5   wind components in x-, y- and z-directions at 10 Hz (see Figure 5). Fifteen-minute averaged values were calculated for wind
speed, wind direction, friction velocity, temperature, stability and turbulence intensity.

2.4 Measurement of GEM flux

Atmosphere-surface fluxes of GEM were measured using the REA technique proposed by Businger and Oncley (1990),
where the vertical turbulent transported flux is estimated from:

10   $F = b \; \sigma_w (\overline{c_{up}} - \overline{c_{down}})$,   (1)

When applying the REA technique, slower responding sensors can be used instead of an eddy covariance technique where
faster responding sensors are required. In eq. (1), b is a proportionality factor (the Businger coefficient) which can be
experimentally determined from sensible heat or another scalar flux; σ_w is the standard deviation of the vertical wind speed;
the overbar denotes a mean; and c_{up} and c_{down} are gas concentration in updrafts and downdrafts, respectively. Separation of
15   updrafts (c_{up}) and downdrafts (c_{down}) is obtained by the sonic anemometer and fast shifting valves, which separates the
airstream according to the direction of fluctuations in the vertical wind velocity.

The REA technique proposed by Businger and Oncley (1990) uses a constant flow rate accounted for by the addition of the
Businger coefficient, discussed extensively elsewhere(e.g. (Gao, 1995;Gronholm et al., 2008;Tsai et al., 2012)). A constant
value for b can be used, but it is preferable to determine b from site to site from other scalars like CO_2 or temperature under
20   the assumption of scalar similarity (Gao, 1995).

Often a wind-controlled "deadband" is introduced to avoid sampling of eddies with a vertical velocity close to zero. A
threshold above or below zero indicates this deadband, and the magnitude of the fluctuations of the vertical wind velocity
must be larger than this threshold to be collected. This also decreases the switching frequency of the valves by removing
many small fluctuations. As a consequence, the deadband will increase the concentration difference between updrafts and
25   downdrafts, hence b is reduced to compensate for the increased difference (Ammann and Meixner, 2002).

The overall system is shown in Figure 5, the system consists of two automated Hg vapor analyzers (Tekran, model 2537X)
are used to measure the GEM concentrations in updrafts and downdrafts, respectively. Data from the two Hg analyzers was
compiled on a PC inside Flyger's hut. The sampling inlets are located 5.69 m above ground. Osterwalder et al. (2016) and
Zhu et al. (2015b) describe the advantages of using dual inlets, where temporally synchronous concentration determination
30   of updrafts and downdrafts is the most obvious advantage. The Teflon tubes were heated to 50°C and each tube is connected
to a three-way valve, which can either collect sample air or zero air. The zero air was delivered from a zero air generator in

excess to the valves when not sampling. A CompactRIO processor (cRIO-9033, National Instruments) sets the position of the valves according to the vertical wind velocity measured with the ultrasonic anemometer. The software LabVIEW (National Instruments) was embedded on the CompactRIO processor with a real time module and a programmable FPGA for high-speed control directly in the hardware. This allowed control of valve positions and collection of data from the ultrasonic

5 anemometer.

The REA system was mounted on a boom on top of Flyger's hut. The boom was placed at the edge of the roof and directed towards the prevailing wind direction in order to minimize flow distortion from the hut.

The standard deviation of the vertical wind speed was obtained from previous wind measurements at Station Nord and used for selection of the deadband range to yield a robust b (Held et al., 2008;Ruppert et al., 2006). Thus, a fixed deadband of

10 ± 0.076 m/s is applied to all the data. Correction for dilution according to the opening times of the valves is performed according to (Sommar et al., 2013):

$$C_{up} = \frac{[c_{up} - c_{zero\,air}(1-\alpha_{up})]}{\alpha_{up}} \; and \; C_{down} = \frac{[c_{down} - c_{zero\,air}(1-\alpha_{down})]}{\alpha_{down}}, \tag{2}$$

where c_{up} and c_{down} refers to the GEM concentration in updrafts (c_{up}) or downdrafts (c_{down}); $c_{zero\,air}$ is the GEM concentration in the zero air delivered to the valves. α_{up} and α_{down} refers to the fraction of time where the updrafts (α_{up}) or downdrafts

15 (α_{down}) are collected.

Tekran 2537 models are based on pre-concentration of Hg on gold cartridges followed by thermal desorption in a flow of inert argon gas, and Hg detection by Cold Vapor Atomic Fluorescence Spectrometry (CVAFS). UV light (253.7 nm) excites Hg atoms, which emit the absorbed energy by fluorescence. Collection on gold traps, thermal desorption and CVAFS is an accurate method to measure Hg content in the air. The detection limit is 0.1 ng m^{-3} (Ma et al., 2015). The sampling interval is

20 15 minutes with a flow rate of 1.5 L min^{-1} and auto calibration every 25 hours. Skov et al. (2004) estimate the reproducibility to be within 20% (95% confidence interval) for two Tekran mercury analyzers measuring above 0.5 ng m^{-3}.

2.5 CO$_2$ flux determination for calculation of b

Close to the REA flux system, an enclosed CO$_2$ gas analyzer (LI-7200, LI-COR Inc.) was mounted on the boom with the inlet directly below the ultrasonic anemometer 6.08 m above ground and above the GEM sample inlets. The gas analyzer

25 measures CO$_2$ and H$_2$O concentration at 10 Hz to derive the EC flux of CO$_2$ and H$_2$O. The CompactRIO compiles all data from the gas analyzer, valve positions and meteorological data from the REA system. The flux of CO$_2$ was measured in order to determine b from the CO$_2$ flux and back-calculations of CO$_2$ concentration in updrafts and downdrafts in each measuring interval (Gao, 1995;Ruppert et al., 2006).

For an ideal Gaussian joint probability distribution of the vertical wind speed and the scalar concentration, b has a well-

30 defined value of 0.627 (Wyngaard and Moeng, 1992). However, experimentally determined b's for fluxes of heat, moisture and CO$_2$ typically range from 0.51 to 0.62 (e.g. (Katul et al., 1996)). If b in a given experiment differs too much from the

Atmospheric
Chemistry
and Physics
Discussions

expected value, the probability distribution is likely to differ from the Gaussian distribution, thus in the present experiment data was discarded in periods where b derived from T or CO_2 was below 0.4 or above 0.8.

Meteorological conditions or parameters, such as temperature, wind direction and speed, heat fluxes, relative humidity, pressure, and water vapor were measured for further analysis of the GEM fluxes. The Monin-Obukhov length (L) was

5   calculated in order to estimate stability, as atmospheric stratification is expected to affect the surface exchange. The shape of the theoretical co-spectra (Kaimal et al., 1972), is a function of stability, where the uncertainties are smaller for neutral conditions ($z/L \approx 0$). Therefore, data was discarded if z/L was below -1.5 or above 1.5 in order to remove ambiguous data. Furthermore, wind speeds below two m s^{-1} were discarded in order to have a well-developed turbulence flow. After data filtration, 26% of the total 1653 measurements were approved during the campaign.

10 The b values are derived from EC and REA flux of CO_2. For each interval, b is used to determine the REA flux of GEM. This correction is anchored in statistical assumptions of zero mean of the fluctuations from EC. We estimate that the uncertainty of b is << 10% and is thus assumed to be insignificant. Hence, the flux estimate is determined from the uncertainty of the two concentration determinations $\sqrt{0.1^2 + 0.1^2} = 0.14$ and the uncertainty of the flux becomes 28% at a 95% confidence interval. The uncertainty of the GEM concentrations is 10% above 0.5 ng m^{-3} (Skov et al., 2004).

15 **3 Results and discussion**

Fluxes of GEM and GEM concentrations are shown in Figures 7a and 7b. Principally, we found GEM emission (positive fluxes) and a net mean emission of 8.9 ng m^{-2} min^{-1} over the 20 days. The largest measured deposition (negative flux) was 8.0 ng m^{-2} min^{-1}, whereas the largest emission was 190.0 ng m^{-2} min^{-1}.

The measurements were started when depletion was already present and, as seen in Figure 7a and Figure 7b, depletion (low

20 GEM concentration during April 23-25 and May 2-5) was followed by GEM emission as observed by Brooks et al. (2006), supporting that GEM is reemitted after AMDEs. The results correspond to the general understanding that GEM is initially removed rapidly. This removal is most likely due to photolytic oxidation to GOM, which, contrary to GEM, has a very low surface resistance (Skov et al., 2006) and thus deposits relatively quickly. After deposition, we speculate that GOM is reduced photolytically to GEM in the surface snow followed by reemission. In accordance with earlier observations, this

25 implies that a predominant fraction of the downward flux of Hg is in the form of GOM during AMDEs (Skov et al. 2006, Brooks et al. 2006). GOM is reduced at the snow surface when the temperature increases (Ferrari et al., 2008). This leads to increased reemission of GEM causing GEM in the atmosphere to again increase. This observation is in agreement with observations from Barrow, Alaska (Skov et al. 2006, Brooks et al. 2006) where GOM fluxes were measured together with gradients of GEM and ozone. However, part of the increase in GEM can also be explained by long-range transportation.

30 Trajectory calculations of air mass transport show downward mixing from higher elevations (Figure 3a), but in order to obtain an upward surface flux the concentration in the snow must be higher than in the atmosphere. We observed a clear

Atmospheric
Chemistry
and Physics
Discussions

diurnal pattern for the radiation intensity with the maximum at noon and the minimum at midnight, but these diurnal variations seem not to influence the GEM flux or concentration.

The rapid increase in GEM flux on April 30 was a unique situation. At that time, the pressure dropped suddenly from 1032 hPa to 1013 hPa and increased again to about 1025 hPa. During this abrupt GEM emission event, latent and sensible heat

5 fluxes decreased rapidly and the temperature increased from about -18℃ up to -4℃ before decreasing to -13℃ again. Wind speed reached its maximum-recorded speed for the duration of the campaign during this peak in the GEM flux. At the same time, stability changed from unstable to stable conditions. The observations above indicate that this sudden increase in GEM flux is most likely explained by a sudden change in meteorological conditions and changes in wind flow. All the meteorological parameters are shown in Figure 6a-e and the GEM flux in Figure 7a.

10 It is clear from Figures 6a and 7a, that all large emission events were connected to increased wind speed as would be expected. Increased wind speeds cause a rise in turbulence transport, which leads to increased vertical turbulence flux. The GEM emission on April 28 was followed by an increase in GEM concentration on April 29, which occurred as the stability rapidly changed from stable to unstable conditions. The day before this event, the GEM concentration was stable at around 1 ng m^{-3} and increased threefold as the stability changed. According to trajectory calculations this sudden increase was not

15 caused by mixing from aloft (Figure 3b). This could have occurred as a result of an extremely stratified surface layer directly above the ground where GEM concentration builds up directly over the snow surface, but the buildup concentration is not detected until the layer at the surface is mixed to higher elevation when the stratification becomes unstable. Thus, the atmospheric stability might have significant influence on GEM concentration measurements during AMDEs, causing concentration fluctuations to be falsely interpreted as outliers. According to Osterwalder et al. (2016), GEM REA fluxes

20 were significantly different under stable, unstable and neutral conditions over a snow-covered surface. In the present study, GEM was primarily emitted under neutral and slightly stable conditions, and fluxes close to zero were observed under unstable and neutral conditions. The opposite is observed by Osterwalder et al. (2016) with emission during unstable conditions, a small deposition during stable conditions and deposition during neutral conditions. These differences can be explained by a non-Arctic location and a very different dynamic of GEM.

25 On May 5, a change from stable to unstable conditions occurred simultaneously with an increase in concentration, which could also be explained by inversion of the surface layer as described above. The concentration increase was not as rapid or as large as the previous event, but there was almost no GEM emission in the days leading up to it, which could be explained by the observation that only a small concentration of GEM was build up before the surface layer was inverted. The concentration increase cannot be explained by a mixing from aloft because the trajectory calculations show a constant air

30 mass transport pattern from May 3 to May 6 (Figure 3c and 3d), which should preclude such an event.

According to Steffen et al. (2015), the photochemical reduction of GOM in snow – and thus the reemission of GEM – is temperature dependent. The highest temperatures were found during events with the largest emissions, as seen in Figures 6b and 7a. This behavior is not found for CO_2 flux, where the fluxes are independent of temperature but does correlate with wind and stability, thus we argue that stability and wind variations can be ruled out as the causes of the changes in GEM

Atmospheric
Chemistry
and Physics
Discussions

emissions presented here. Apparently, there is some correlation between CO_2 and GEM, but the reason for this correlation is unknown and we speculate that chemical reactions or bacterial activity in the snow could be partially responsible for this result; further research regarding this is needed. At low temperature (< -20 ℃) the flux of GEM was near zero. Low temperatures are required for the occurrence of AMDE (< -4 ℃) (Lindberg et al., 2002;Skov et al., 2004), at which point

5   GEM is oxidized to GOM. This indicates that GEM is so easily oxidized to GOM at lower temperatures (< -20 ℃) that GEM falls below detection limit. Ozone and GEM depletion are correlated during AMDEs possibly due to reactions with Br, and low temperatures favor the reaction between Br and Hg^0 (Goodsite et al., 2004, 2012;Skov et al., 2004;Schroeder et al., 1998). Further, Hg(II) are water-soluble, hence it is assumed that reduction of deposited Hg takes place in the water phase (Steffen et al., 2015), which is followed by emission of the more volatile GEM. It is possible that the temperature

10   dependence observed here is due to increased water content in the snowpack. Heating of the surface (i.e. downward sensible heat flux) and upward latent heat flux occurred on April 27 during the first larger GEM emission event, supporting the temperature- and water- dependency hypothesis. The temperature dependence of GEM during AMDEs is illustrated in Figure 8. Similarly, in the sub-arctic Dommergue et al. (2003) showed that melting snow emits more GEM than at lower snow temperatures.

15   Chamber measurements are enclosure methods, and therefore run the risk of potentially changing temperature, humidity, radiation, etc. (Fowler et al., 2001). Micrometeorological methods, such as REA and AGM, are non-invasive, and are thus more appropriate for comparing the results of the present study with other non-invasive methods. Our findings do not agree with Cobbett et al. (2007) and Manca et al. (2013), as we found few negative fluxes of GEM and a large net emission of GEM during the campaign despite the potential for long-range transported GEM between April 25 and April 28. However,

20   Brooks et al. (2006) report a small reemission of GEM with a net gain of mercury in the snow over a two-week period during March-April 2003 at Barrow, Alaska. A net emission of GEM was found in the present study, as well as in those conducted by Brooks et al. (2006) and Steen et al. (2009), but the net GEM flux evident in the present study is much higher than others have observed. A study by Ferrari et al. (2004) was performed at the same location as the present study, but the range of the fluxes found were more than three orders of magnitude lower than presented here. This could be due to higher wind speeds

25   and concentration levels during the present study. Despite the difference in magnitudes of fluxes, GEM depletion was observed in all three studies. Brooks et al. (2006) estimated the GOM flux from surface resistance models based on results in Skov et al. (2006), while gradient measurements were used to estimate the GEM flux, thus the difference in the estimated fluxes can also be explained by differences in the methods used. Measurements by Cobbett et al. (2007) from April to June in Alert, Canada showed zero net flux. The most significant fluxes observed during polar day were found in early June when

30   and where the soil was visible, which was never the case during the present study's campaign. Manca et al. (2013) found a net deposition at Ny Ålesund, Svalbard from April to May with significant depositions and emissions, which can be explained by the location, since Ny Ålesund is located at open seawater and thus it is not expected that any local AMDEs would take place because AMDEs are related to sea ice and snow surfaces. The measurements by Manca et al. (2013) were carried out over a snow-covered surface, but the processes involved were different due to the location at open water. During

the present study, the air masses recorded derived mainly from sea ice during the depletion events (Figures 4a and 4b) in spite of the local SW winds.

As mentioned earlier, we speculate that strong stable conditions can result in GEM buildup directly above the surface, similar to CO_2 storage over forested sites (Yang et al., 2007). Surface emission of GEM into a relatively shallow layer of air

5   will result in its higher concentration close to the ground. If the measurement height is above the "ground surface layer" the measured flux will increase when the stability changes and mix the air directly above the surface to higher elevations. Brooks et al. (2006), Cobbett et al. (2007) and Manca et al. (2013) all used the flux gradient method to determine GEM flux, and the different results obtained could be due to the flux measurement techniques used. Using the gradient method, flux is estimated from concentration measurements at different heights. Strong stratification with GEM buildup near the surface will

10   likely result in a non-constant flux layer, violating a basic assumption for the flux gradient method.

The study sites in the present study and in the studies by Brooks et al. (2006), Cobbett et al. (2007) and Manca et al. (2013) differ significantly in terms of orography and meteorology, which have an effect on the fluxes. Theoretical studies by Goodsite et al. (2004) and Goodsite et al. (2012) show that GEM removal is driven by chemical reaction with Br and increases with decreasing temperature. Differences in locations between research sites undoubtedly affect the concentrations

15   of GEM. Important parameters are e.g. temperature, Br and origin of air masses. The wind direction in the present study was primarily from SW, caused by katabatic winds from the local Flade Isblink glacier; however this is merely the source of the local wind and most air masses in the study area overall are derived from sea-ice covered surfaces according to the trajectory calculations (see Figures 3 and 4). As mentioned, atmospheric stability influences the observed GEM fluxes (Osterwalder et al., 2016) and different stability conditions between sites could explain the differences in fluxes found by Cobbett et al.

20   (2007) and Manca et al. (2013). Overall, our results suggest that variations in GEM concentrations and fluxes are much more variable than previously assumed.

4 Conclusion

Mercury is primarily transported in the atmosphere in the form of GEM and it is ubiquitous in the atmosphere. Fluxes of GEM have been measured at Villum Research Station, Station Nord, in the high Arctic of north Greenland over snow-

25   covered surfaces from April 23 to May 12, 2016 with a REA system utilizing dual inlets and dual detectors.

This work showed an average GEM emission of 8.9 ng m^{-2} min^{-1} during the 20-day research campaign, during which several AMDEs were observed. A maximum deposition of 8.0 ng m^{-2} min^{-1} and a maximum emission of 190 ng m^{-2} min^{-1} were recorded. The results of this study support the general understanding of the AMDE mechanisms where GEM oxidation is followed by deposition of GOM, which is partly reduced to GEM and reemitted into the atmosphere. Furthermore, the data

30   supports the hypothesis that temperature (heating of the surface) and water present in the snow is influencing GEM formation and reemission after depletion.

The observed fluxes and concentrations are related to meteorological conditions and comparing concentrations and fluxes found at other high-latitude sites reveals wide variation between sites. However, these comparisons imply that GEM fluxes and concentrations can be rather heterogeneously dispersed in the Arctic atmosphere due to the complex meteorological flows and stratification.

5 Further studies on this heterogeneity, including potential inversion at the surface and mixing from aloft, are needed, as are studies of fluxes of both GEM and GOM adjacent with measurements of the energy budget and controlling parameters extant in snow pack.

Competing interests

The authors declare that they have no conflict of interest.

Acknowledgements

References

AMAP: AMAP Assessment 2011: Mercury in the Arctic. Arctic Monitoring and Assessment Programme (AMAP), Oslo, Norway, xiv + 193 pp, 2011.

Ammann, C., and Meixner, F. X.: Stability dependence of the relaxed eddy accumulation coefficient for various scalar quantities, Journal of Geophysical Research, 107, 10.1029/2001jd000649, 2002.

Angot, H., Dastoor, A., Simone, F. D., Gårdfeldt, K., Gencarelli, C. N., Hedgecock, I. M., Langer, S., Magand, O., Mastromonaco, M. N., and Nordstrøm, C.: Chemical cycling and deposition of atmospheric mercury in polar regions: review of recent measurements and comparison with models, Atmospheric Chemistry and Physics, 16, 10735-10763, 2016.

Berg, T., Sekkesæter, S., Steinnes, E., Valdal, A., and Wibetoe, G.: Springtime depletion of mercury in the European Arctic as observed at Svalbard, Science of The Total Environment, 304, 43-51, http://dx.doi.org/10.1016/S0048-9697(02)00555-7, 2003.

Berg, T., Pfaffhuber, K. A., Cole, A. S., Engelsen, O., and Steffen, A.: Ten-year trends in atmospheric mercury concentrations, meteorological effects and climate variables at Zeppelin, Ny-Ålesund, Atmos. Chem. Phys., 13, 6575-6586, 10.5194/acp-13-6575-2013, 2013.

Brooks, S. B., Saiz-Lopez, A., Skov, H., Lindberg, S. E., Plane, J. M. C., and Goodsite, M. E.: The mass balance of mercury in the springtime arctic environment, Geophysical Research Letters, 33, 10.1029/2005gl025525, 2006.

Businger, J. A., and Oncley, S. P.: Flux Measurement with Conditional Sampling, Journal of Atmospheric and Oceanic Technology, 349 - 352, 1990.

Christensen, J., Brandt, J., Frohn, L., and Skov, H.: Modelling of mercury in the Arctic with the Danish Eulerian Hemispheric Model, Atmospheric Chemistry and Physics, 4, 2251-2257, 2004.

5   Cobbett, F. D., Steffen, A., Lawson, G., and Van Heyst, B. J.: GEM fluxes and atmospheric mercury concentrations (GEM, RGM and) in the Canadian Arctic at Alert, Nunavut, Canada (February–June 2005), Atmospheric Environment, 41, 6527-6543, http://dx.doi.org/10.1016/j.atmosenv.2007.04.033, 2007.

Cobos, D. R., Baker, J. M., and Nater, E. A.: Conditional sampling for measuring mercury vapor fluxes, Atmospheric Environment, 36, 4309-4321, http://dx.doi.org/10.1016/S1352-2310(02)00400-4, 2002.

10 Dastoor, A. P., Davignon, D., Theys, N., Van Roozendael, M., Steffen, A., and Ariya, P. A.: Modeling Dynamic Exchange of Gaseous Elemental Mercury at Polar Sunrise, Environmental Science & Technology, 42, 5183-5188, 10.1021/es800291w, 2008.

Dommergue, A., Ferrari, C. P., Gauchard, P. A., Boutron, C. F., Poissant, L., Pilote, M., Jitaru, P., and Adams, F. C.: The fate of mercury species in a sub-arctic snowpack during snowmelt, Geophysical research letters, 30, 2003.

15 Ebinghaus, R., Kock, H. H., Temme, C., Einax, J. W., Löwe, A. G., Richter, A., Burrows, J. P., and Schroeder, W. H.: Antarctic Springtime Depletion of Atmospheric Mercury, Environmental Science & Technology, 36, 1238-1244, 10.1021/es015710z, 2002.

Faïn, X., Helmig, D., Hueber, J., Obrist, D., and Williams, M. W.: Mercury dynamics in the Rocky Mountain, Colorado, snowpack, Biogeosciences, 10, 3793-3807, 2013.

20 Ferrari, C. P., Dommergue, A., Boutron, C. F., Skov, H., Goodsite, M., and Jensen, B.: Nighttime production of elemental gaseous mercury in interstitial air of snow at Station Nord, Greenland, Atmospheric Environment, 38, 2727-2735, http://dx.doi.org/10.1016/j.atmosenv.2004.02.023, 2004.

Ferrari, C. P., Gauchard, P.-A., Aspmo, K., Dommergue, A., Magand, O., Bahlmann, E., Nagorski, S., Temme, C., Ebinghaus, R., Steffen, A., Banic, C., Berg, T., Planchon, F., Barbante, C., Cescon, P., and Boutron, C. F.: Snow-to-air
25 exchanges of mercury in an Arctic seasonal snow pack in Ny-Ålesund, Svalbard, Atmospheric Environment, 39, 7633-7645, http://dx.doi.org/10.1016/j.atmosenv.2005.06.058, 2005.

Ferrari, C. P., Padova, C., Faïn, X., Gauchard, P.-A., Dommergue, A., Aspmo, K., Berg, T., Cairns, W., Barbante, C., Cescon, P., Kaleschke, L., Richter, A., Wittrock, F., and Boutron, C.: Atmospheric mercury depletion event study in Ny-Alesund (Svalbard) in spring 2005. Deposition and transformation of Hg in surface snow during springtime, Science of The
30 Total Environment, 397, 167-177, http://dx.doi.org/10.1016/j.scitotenv.2008.01.064, 2008.

Fowler, D., Coyle, M., Flechard, C., Hargreaves, K., Nemitz, E., Storeton-West, R., Sutton, M., and Erisman, J.-W.: Advances in micrometeorological methods for the measurement and interpretation of gas and particle nitrogen fluxes, Plant and Soil, 228, 117-129, 2001.

Gao, W.: The vertical change of coefficient b, used in the relaxed eddy accumulation method for flux measurement above
35 and within a forest canopy, Atmospheric Environment, 2339-2347, 1995.

Goodsite, M. E., Plane, J. M. C., and Skov, H.: A Theoretical Study of the Oxidation of Hg0 to HgBr2 in the Troposphere, Environmental Science & Technology, 38, 1772-1776, 10.1021/es034680s, 2004.

Goodsite, M. E., Plane, J. M. C., and Skov, H.: Correction to A Theoretical Study of the Oxidation of Hg0 to HgBr2 in the Troposphere, Environmental Science & Technology, 46, 5262-5262, 10.1021/es301201c, 2012.

40 Gronholm, T., Haapanala, S., Launiainen, S., Rinne, J., Vesala, T., and Rannik, U.: The dependence of the beta coefficient of REA system with dynamic deadband on atmospheric conditions, Environ Pollut, 152, 597-603, 10.1016/j.envpol.2007.06.071, 2008.

Hausmann, M., and Platt, U.: Spectroscopic measurement of bromine oxide and ozone in the high Arctic during Polar Sunrise Experiment 1992, Journal of Geophysical Research: Atmospheres, 99, 25399-25413, 1994.

45 Held, A., Patton, E., Rizzo, L., Smith, J., Turnipseed, A., and Guenther, A.: Relaxed Eddy Accumulation Simulations of Aerosol Number Fluxes and Potential Proxy Scalars, Boundary-Layer Meteorology, 129, 451-468, 10.1007/s10546-008-9327-5, 2008.

Holmes, C. D., Jacob, D. J., and Yang, X.: Global lifetime of elemental mercury against oxidation by atomic bromine in the free troposphere, Geophysical Research Letters, 33, 10.1029/2006GL027176, 2006.

Kaimal, J. C., Wyngaard, J. C., Izumi, Y., and Coté, O. R.: Spectral characteristics of surface-layer turbulence, Quarterly Journal of the Royal Meteorological Society, 563-589, 1972.

Katul, G. G., Finkelstein, P. L., Clarke, J. F., and Ellestad, T. G.: An Investigation of the Conditional Sampling Method Used to Estimate Fluxes of Active, Reactive, and Passive Scalars, Journal of Applied Meteorology, 35, 1835-1845, 10.1175/1520-0450(1996)035<1835:AIOTCS>2.0.CO;2, 1996.

Lalonde, J. D., Poulain, A. J., and Amyot, M.: The Role of Mercury Redox Reactions in Snow on Snow-to-Air Mercury Transfer, Environmental Science & Technology, 36, 174-178, 10.1021/es010786g, 2002.

Lindberg, S. E., Brooks, S., Lin, C. J., Scott, K. J., Landis, M. S., Stevens, R. K., Goodsite, M., and Richter, A.: Dynamic Oxidation of Gaseous Mercury in the Arctic Troposphere at Polar Sunrise, Environmental Science & Technology, 36, 1245-1256, 10.1021/es0111941, 2002.

Ma, M., Wang, D., Du, H., Sun, T., Zhao, Z., and Wei, S.: Atmospheric mercury deposition and its contribution of the regional atmospheric transport to mercury pollution at a national forest nature reserve, southwest China, Environmental Science and Pollution Research, 22, 20007-20018, 10.1007/s11356-015-5152-9, 2015.

Manca, G., Ammoscato, I., Esposito, G., Ianniello, A., Nardino, M., and Sprovieri, F.: Dynamics of snow-air mercury exchange at Ny Ålesund during springtime 2011, E3S Web of Conferences, 1, 2013.

Osterwalder, S., Fritsche, J., Alewell, C., Schmutz, M., Nilsson, M. B., Jocher, G., Sommar, J., Rinne, J., and Bishop, K.: A dual-inlet, single detector relaxed eddy accumulation system for long-term measurement of mercury flux, Atmos. Meas. Tech., 9, 509-524, 10.5194/amt-9-509-2016, 2016.

Pandey, S. K., Kim, K.-H., and Brown, R. J. C.: Measurement techniques for mercury species in ambient air, Trends in Analytical Chemistry, 30, 899-917, 10.1016/j.trac.2011.01.017, 2011.

Rasch, M., Frandsen, E. R., Skov, H., and Hansen, J. L.: Site Manual (Villum Research Station, Station Nord, Greenland), www.villumresearchstation.dk, 2015.

Rolph, G., Stein, A., and Stunder, B.: Real-time Environmental Applications and Display sYstem: READY, Environmental Modelling & Software, 95, 210-228, http://dx.doi.org/10.1016/j.envsoft.2017.06.025, 2017.

Ruppert, J., Thomas, C., and Foken, T.: Scalar Similarity for Relaxed Eddy Accumulation Methods, Boundary-Layer Meteorology, 120, 39-63, 10.1007/s10546-005-9043-3, 2006.

Schroeder, W. H., Anlauf, K. G., Barrie, L. A., Lu, J. Y., Steffen, A., Schneeberger, D. R., and Berg, T.: Arctic springtime depletion of mercury, Nature, 394, 331-332, 1998.

Skov, H., Christensen, J. H., Goodsite, M. E., Heidam, N. Z., Jensen, B., Wåhlin, P., and Geernaert, G.: Fate of Elemental Mercury in the Arctic during Atmospheric Mercury Depletion Episodes and the Load of Atmospheric Mercury to the Arctic, Environmental Science & Technology, 38, 2373-2382, 10.1021/es030080h, 2004.

Skov, H., Brooks, S. B., Goodsite, M. E., Lindberg, S. E., Meyers, T. P., Landis, M. S., Larsen, M. R. B., Jensen, B., McConville, G., and Christensen, J.: Fluxes of reactive gaseous mercury measured with a newly developed method using relaxed eddy accumulation, Atmospheric Environment, 40, 5452-5463, 10.1016/j.atmosenv.2006.04.061, 2006.

Sommar, J., Wängberg, I., Berg, T., Gårdfeldt, K., Munthe, J., Richter, A., Urba, A., Wittrock, F., and Schroeder, W.: Circumpolar transport and air-surface exchange of atmospheric mercury at Ny-Ålesund (79° N), Svalbard, spring 2002, Atmospheric Chemistry and Physics, 7, 151-166, 2007.

Sommar, J., Zhu, W., Shang, L., Feng, X., and Lin, C.-J.: A whole-air relaxed eddy accumulation measurement system for sampling vertical vapour exchange of elemental mercury, 2013, 65, 10.3402/tellusb.v65i0.19940, 2013.

Steen, A. O., Berg, T., Dastoor, A. P., Durnford, D. A., Hole, L. R., and Pfaffhuber, K. A.: Dynamic exchange of gaseous elemental mercury during polar night and day, Atmospheric Environment, 43, 5604-5610, http://dx.doi.org/10.1016/j.atmosenv.2009.07.069, 2009.

Steffen, A., Schroeder, W. H., Bottenheim, J., Narayan, J., and Fuentes, J. D.: Atmospheric mercury concentrations: measurements and profiles near snow and ice surfaces in the Canadian Arctic during Alert 2000, Atmospheric Environment, 36, 2653-2661, http://dx.doi.org/10.1016/S1352-2310(02)00112-7, 2002.

Steffen, A., Douglas, T., Amyot, M., Ariya, P., Aspmo, K., Berg, T., Bottenheim, J., Brooks, S., Cobbett, F., Dastoor, A., Dommergue, A., Ebinghaus, R., Ferrari, C., Gardfeldt, K., Goodsite, M. E., Lean, D., Poulain, A. J., Scherz, C., Skov, H., Sommar, J., and Temme, C.: A synthesis of atmospheric mercury depletion event chemistry in the atmosphere and snow, Atmospheric Chemistry and Physics, 8, 1445-1482, 10.5194/acp-8-1445-2008, 2008.

Steffen, A., Bottenheim, J., Cole, A., Ebinghaus, R., Lawson, G., and Leaitch, W. R.: Atmospheric mercury speciation and mercury in snow over time at Alert, Canada, Atmospheric Chemistry and Physics, 13, 17021-17052, 2014.

Steffen, A., Lehnherr, I., Cole, A., Ariya, P., Dastoor, A., Durnford, D., Kirk, J., and Pilote, M.: Atmospheric mercury in the Canadian Arctic. Part I: a review of recent field measurements, The Science of the total environment, 509-510, 3, 2015.

5   Stein, A. F., Draxler, R. R., Rolph, G. D., Stunder, B. J. B., Cohen, M. D., and Ngan, F.: NOAA's HYSPLIT Atmospheric Transport and Dispersion Modeling System, Bulletin of the American Meteorological Society, 96, 2059-2077, 10.1175/bams-d-14-00110.1, 2015.

Sørensen, A. L., Skov, H., Jacob, D. J., Sørensen, B. T., and Johnson, M. S.: Global Concentrations of Gaseous Elemental Mercury and Reactive Gaseous Mercury in the Marine Boundary Layer, Environmental Science & Technology, 44, 7425–

10   7430, 2010.

Toyota, K., McConnell, J., Staebler, R., and Dastoor, A.: Air–snowpack exchange of bromine, ozone and mercury in the springtime Arctic simulated by the 1-D model PHANTAS–Part 1: In-snow bromine activation and its impact on ozone, Atmospheric Chemistry and Physics, 14, 4101-4133, 2014.

Travnikov, O., Angot, H., Artaxo, P., Bencardino, M., Bieser, J., D'Amore, F., Dastoor, A., De Simone, F., del Carmen

15   Diéguez, M., and Dommergue, A.: Multi-model study of mercury dispersion in the atmosphere: Atmospheric processes and model evaluation, Atmospheric Chemistry and Physics, 17, 5271, 2017.

Tsai, J.-L., Tsuang, B.-J., Kuo, P.-H., Tu, C.-Y., Chen, C.-L., Hsueh, M.-T., Lee, C.-S., Yao, M.-H., and Hsueh, M.-L.: Evaluation of the relaxed eddy accumulation coefficient at various wetland ecosystems, Atmospheric Environment, 60, 336-347, 10.1016/j.atmosenv.2012.06.081, 2012.

20   Valente, R. J., Shea, C., Lynn Humes, K., and Tanner, R. L.: Atmospheric mercury in the Great Smoky Mountains compared to regional and global levels, Atmospheric Environment, 41, 1861-1873, http://dx.doi.org/10.1016/j.atmosenv.2006.10.054, 2007.

Wyngaard, J. C., and Moeng, C.-H.: Parameterizing turbulent diffusion through the joint probability density, Boundary-Layer Meteorology, 60, 1-13, 10.1007/BF00122059, 1992.

25   Yang, B., Hanson, P. J., Riggs, J. S., Pallardy, S. G., Heuer, M., Hosman, K. P., Meyers, T. P., Wullschleger, S. D., and Gu, L. H.: Biases of CO2 storage in eddy flux measurements in a forest pertinent to vertical configurations of a profile system and CO2 density averaging, Journal of Geophysical Research: Atmospheres, 112, 2007.

Zhu, W., Sommar, J., Lin, C. J., and Feng, X.: Mercury vapor air–surface exchange measured by collocated micrometeorological and enclosure methods – Part I: Data comparability and method characteristics, Atmos. Chem. Phys.,

30   15, 685-702, 10.5194/acp-15-685-2015, 2015a.

Zhu, W., Sommar, J., Lin, C. J., and Feng, X.: Mercury vapor air–surface exchange measured by collocated micrometeorological and enclosure methods – Part II: Bias and uncertainty analysis, Atmos. Chem. Phys., 15, 5359-5376, 10.5194/acp-15-5359-2015, 2015b.

Atmospheric
Chemistry
and Physics
Discussions

Figures and tables

Figure 1: Left: Greenland with indication of the largest Natural Reserve in the world (blue) and the position of Station Nord (yellow dot). Right: The northern hemisphere where Station Nord (Nord) also can be seen.
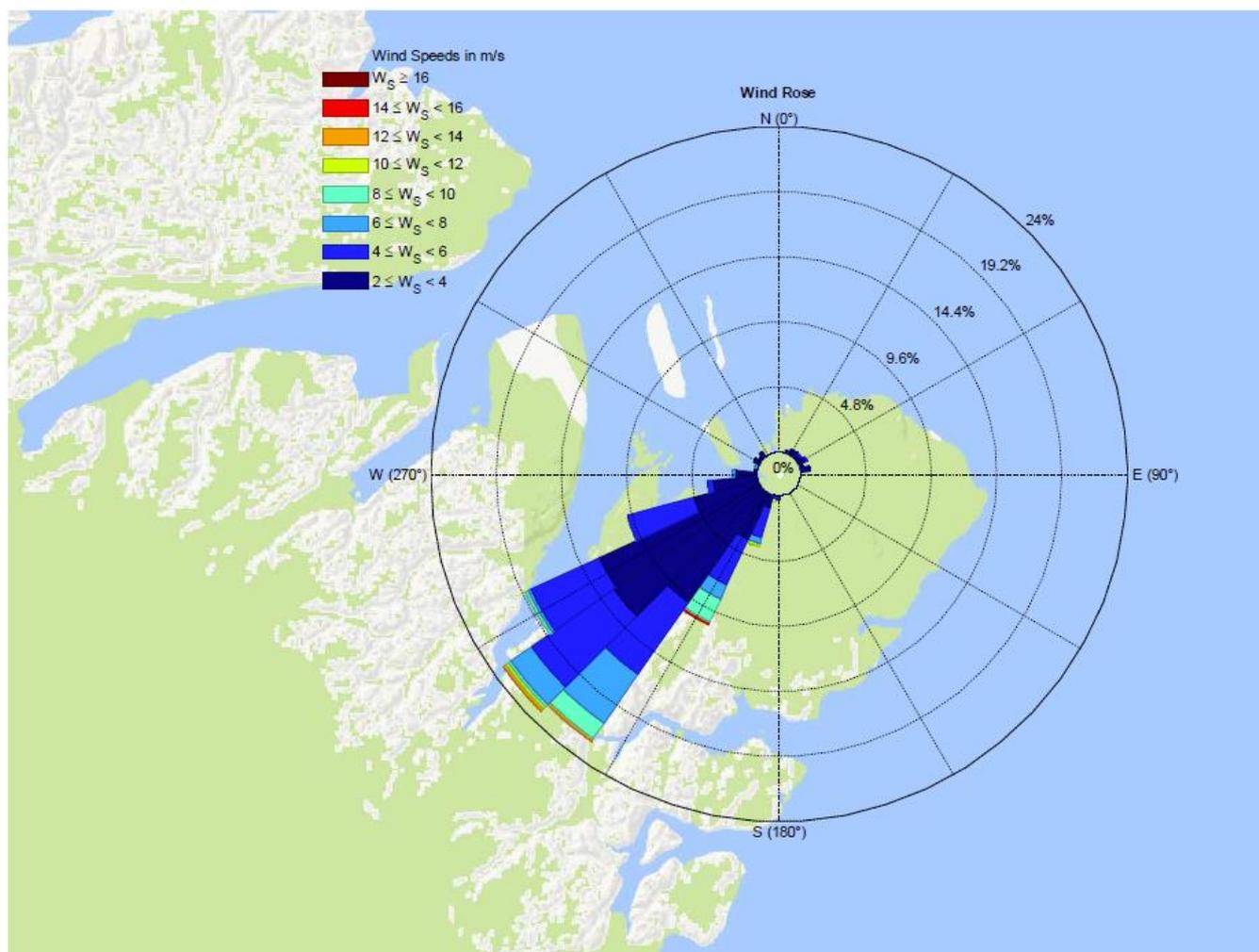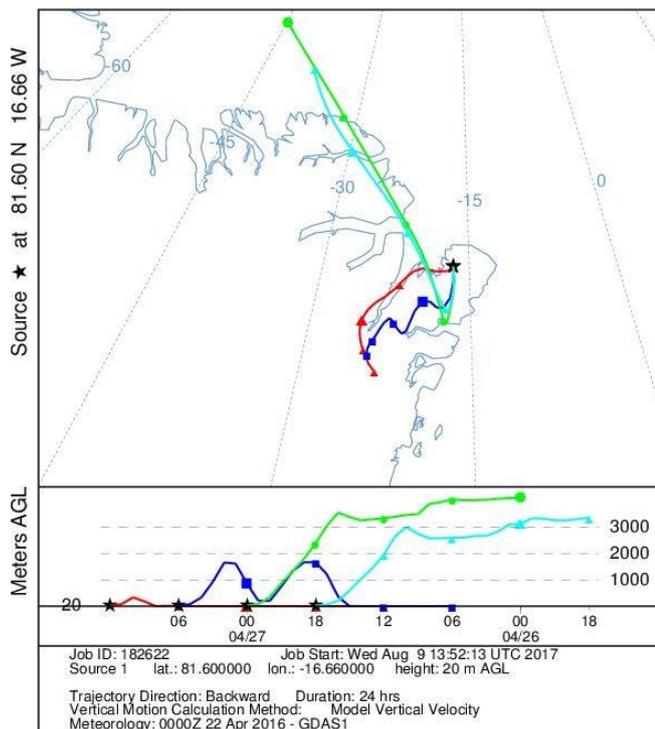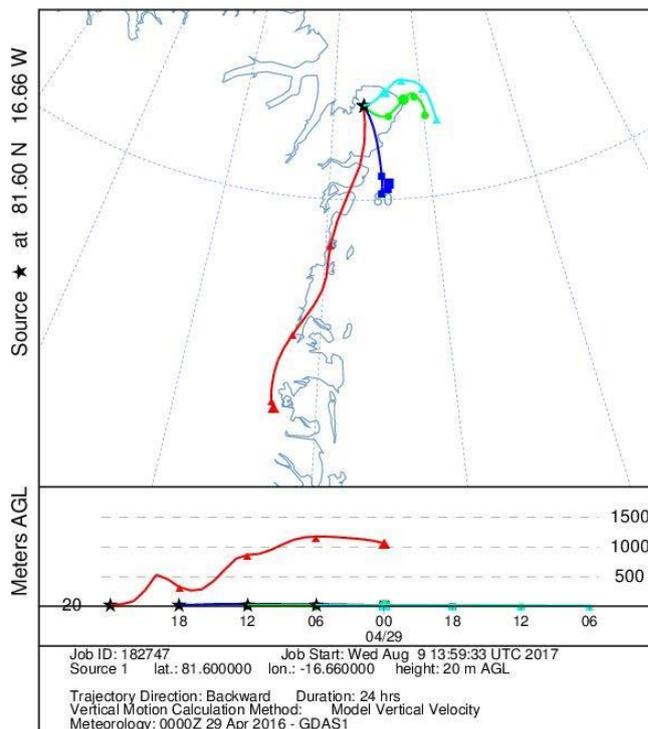
Figure 2: Wind rose centered at Villum Research Station, Station Nord. Length of the bars indicate frequency of the direction and color indicate the wind speed. Units in m s^{-1}.
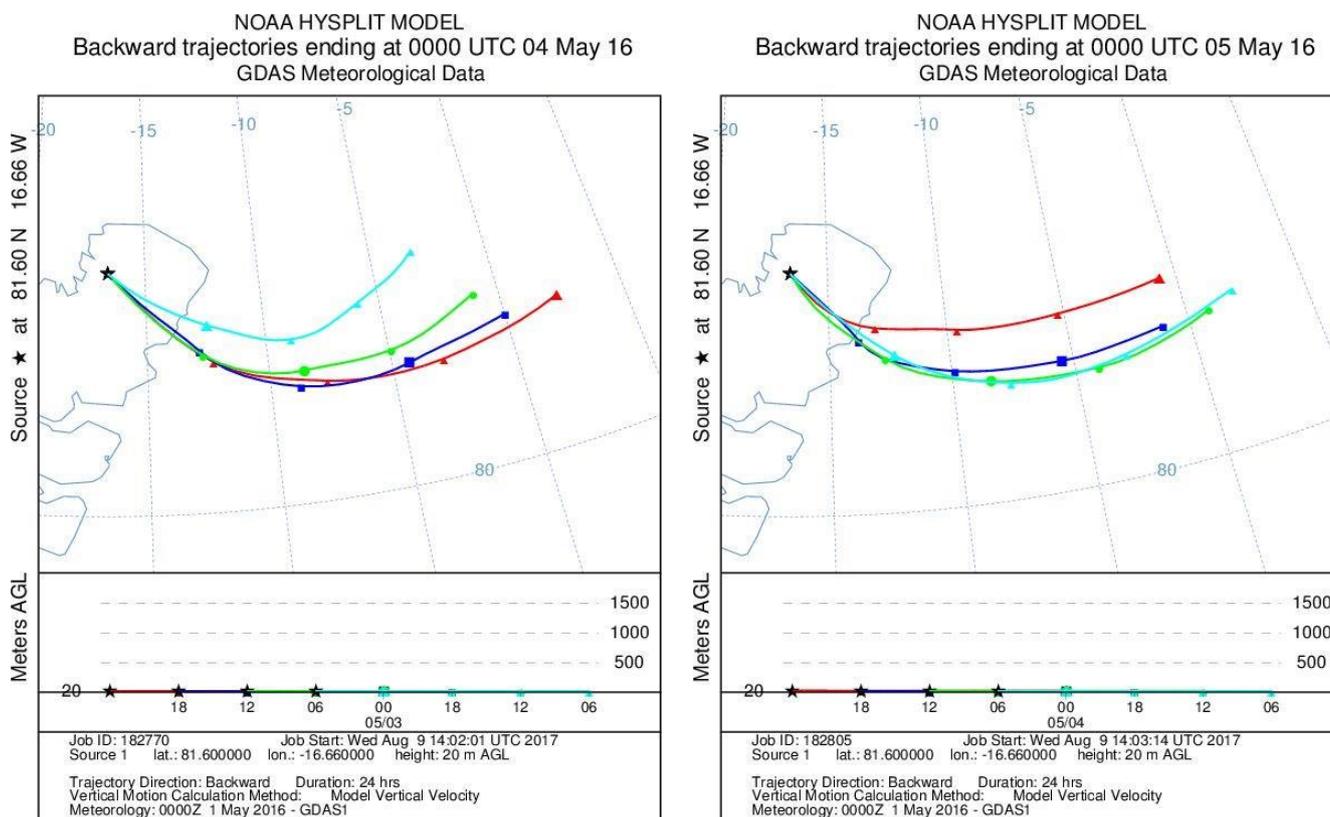
Atmospheric
Chemistry
and Physics
Discussions

Open Access

Figure 3: Backward trajectories for four different days showing the origin of the air masses. All trajectories are 24-hour calculations and each figure show a new trajectory for every 6 hour backward. a) Top left panel, starting April 27, 12:00. b) Top right panel, starting April 30, 00:00. c) Bottom left panel, starting May 4, 00:00. d) Bottom right panel, starting May 5, 00:00.
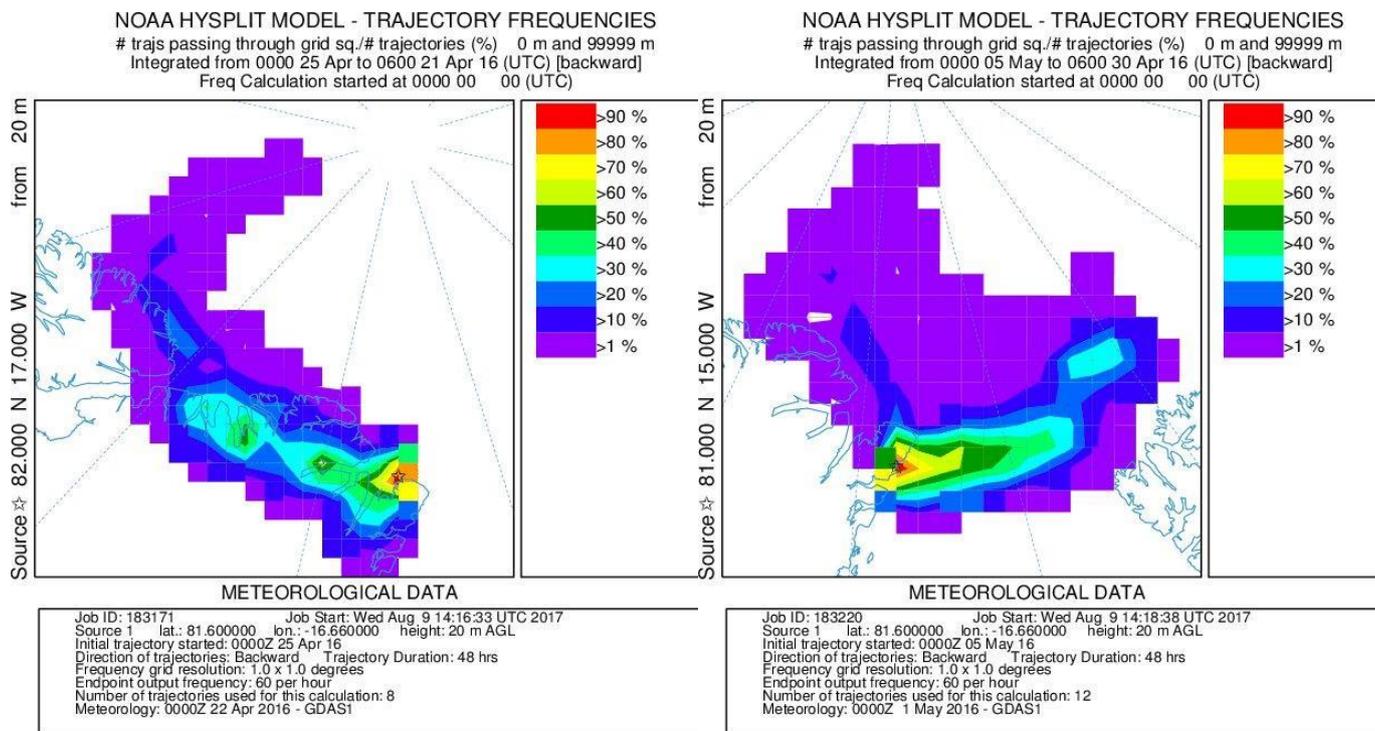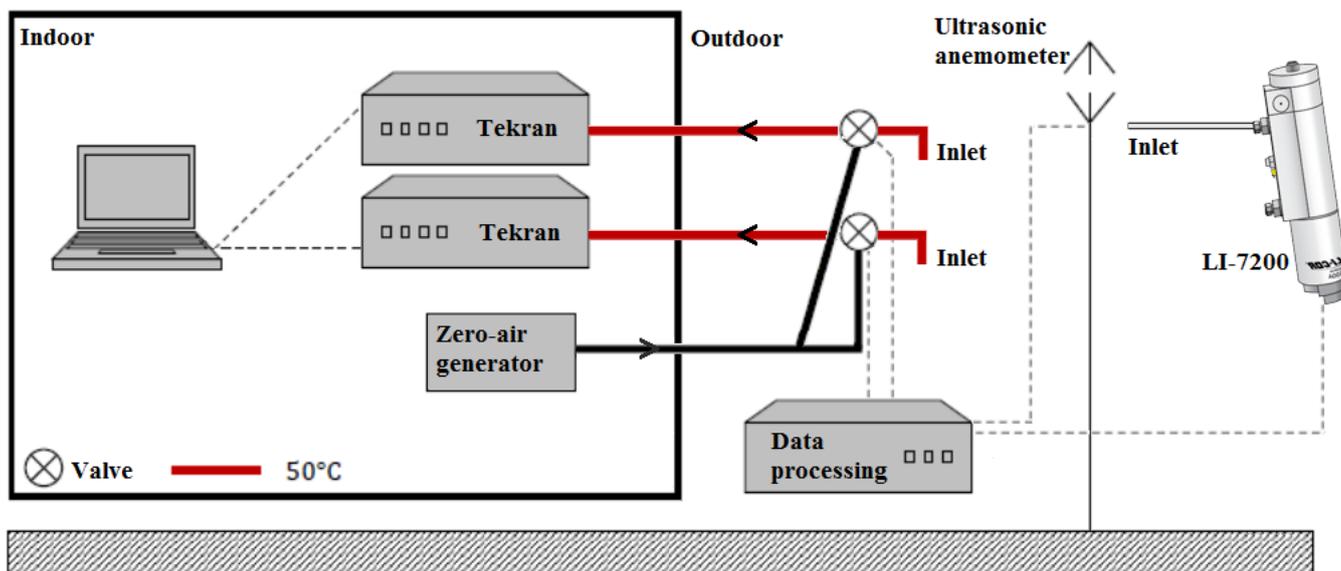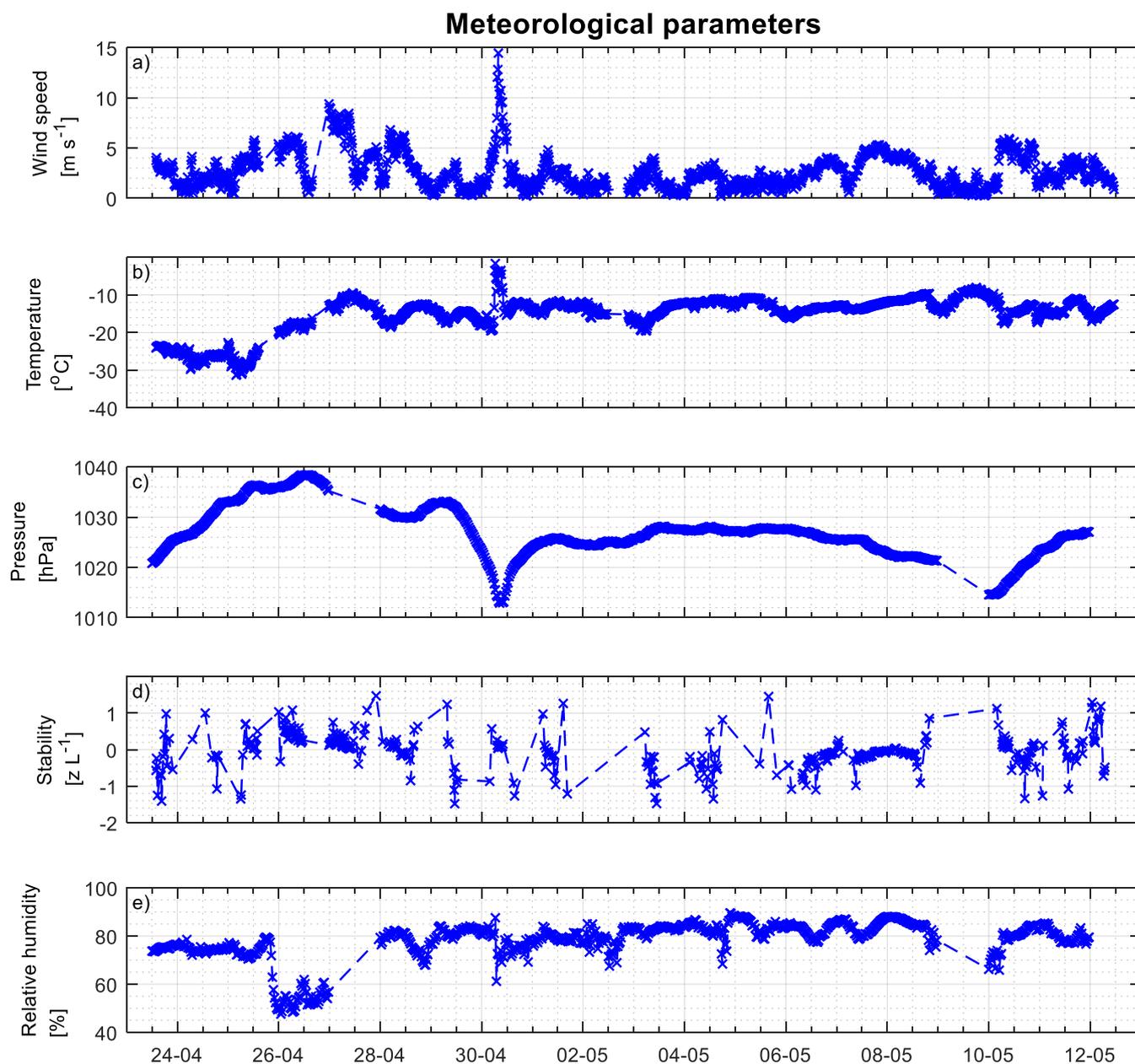
Figure 4: Trajectory frequencies showing the number of trajectories passing through a grid. The resolution is 1 degree. a) Left panel, April 21 to April 25. b) Right panel, April 30 to May 5.

Figure 5: A Schematic representation of the GEM REA system.

Figure 6: Meteorological parameters over time. a) Wind speed in m s⁻¹, b) Temperature in °C, c) Pressure in hPa, d) Stability as z/L, and e) Relative humidity in %.
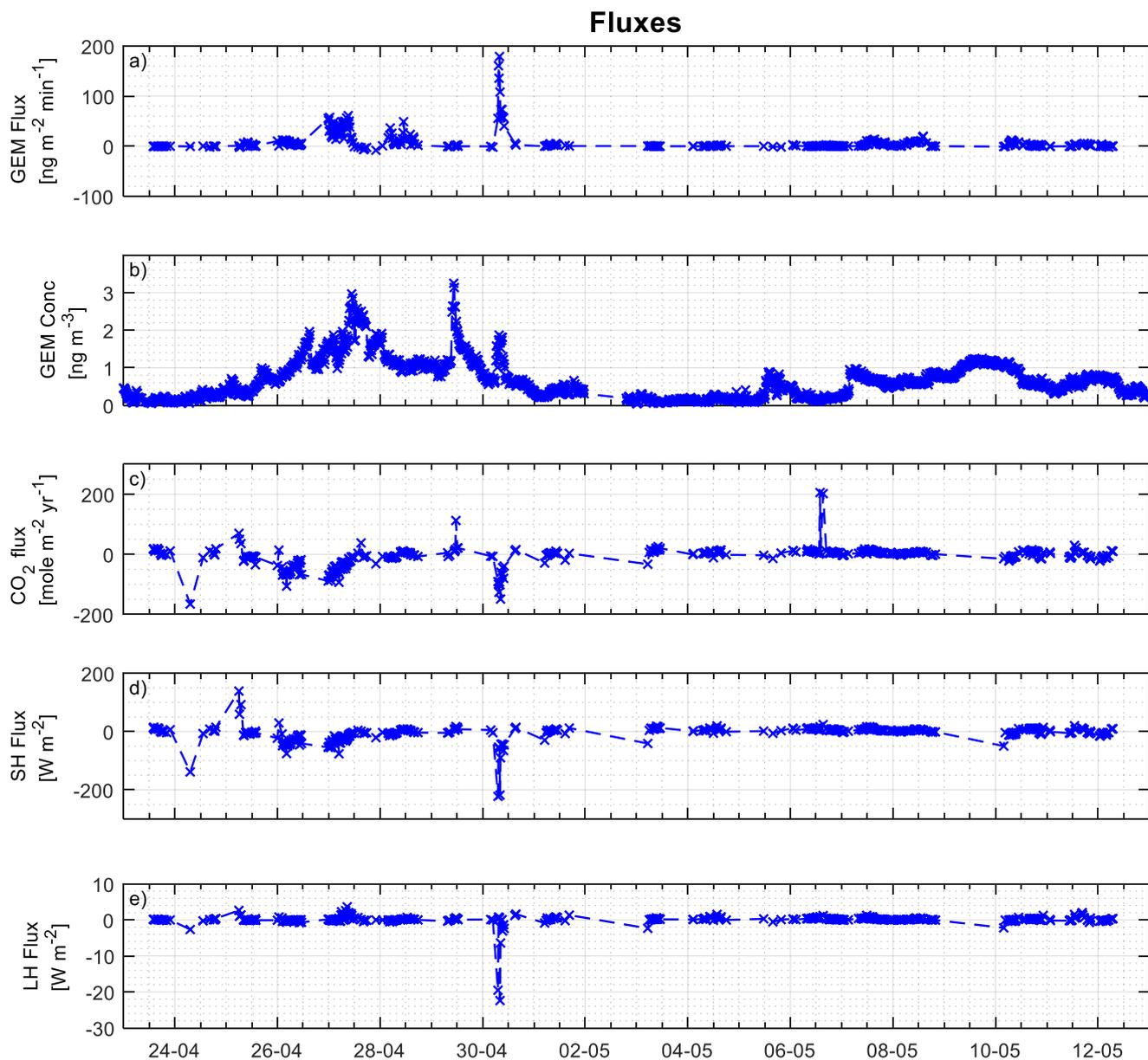
Figure 7: Fluxes and GEM concentration over time. a) GEM flux in ng m^{-2} min^{-1}, b) GEM concentration in ng m^{-3}, c) CO$_2$ flux in mole m^{-2} yr^{-1}, d) Sensible heat flux in W m^{-2}, e) Latent heat flux in W m^{-2}.
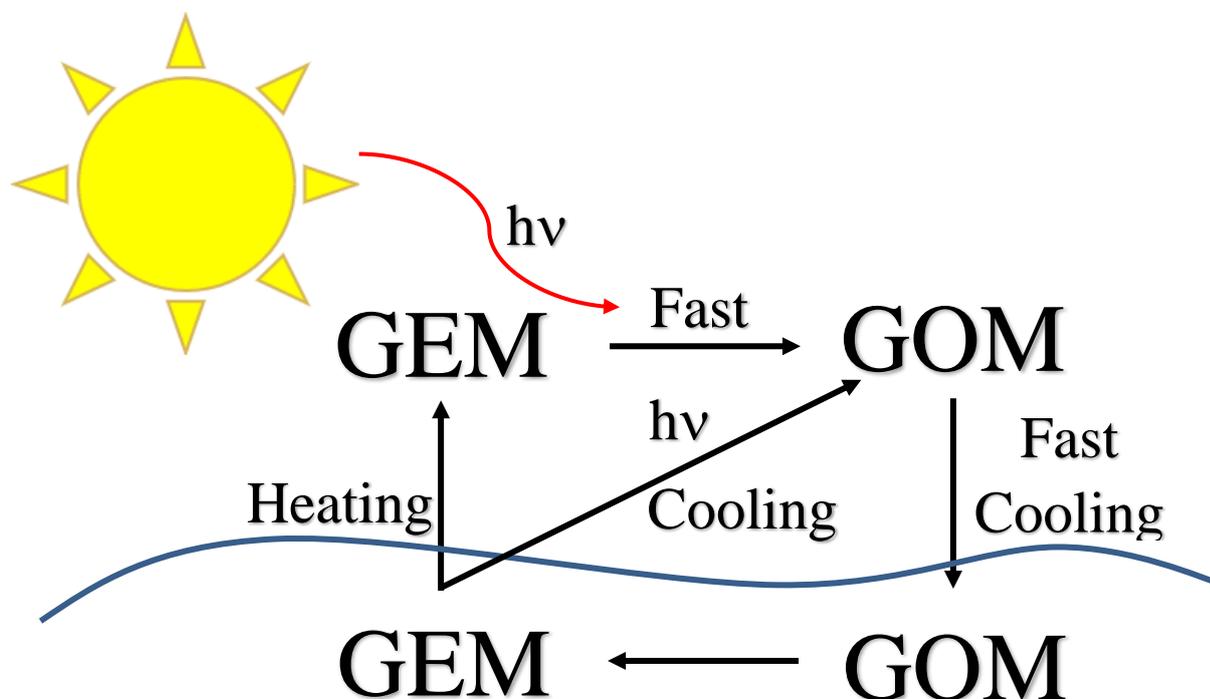
Figure 8: Schematic of possible pathways for GEM and GOM during AMDEs.

Table 1: Summary table over reported GEM fluxes in the Arctic. The units are changed from those within the references for better comparison.

Flux	Site	Method	Reference
Mean: 8.9 ng m^{-2} min^{-1} Range: 8.0-190 ng m^{-2} min^{-1}	Villum Research Station, Station Nord, Greenland	Relaxed eddy accumulation	Present study
Mean: 0.050 ng m^{-2} min^{-1} (in reference: 1.0 µg m^{-2} 14 days^{-1})	Barrow, Alaska	Flux gradient method	Brooks et al. (2006)
Mean: -0.60 ng m^{-2} min^{-1}	Alert, Canada	Flux gradient method	Cobbett et al. (2007)
Mean: -0.004 ng m^{-2} min^{-1}	Ny Ålesund, Svalbard	Flux gradient method	Manca et al. (2013)
Median: 0.12 ng m^{-2} min^{-1}	Ny Ålesund, Svalbard	Flux gradient method	Steen et al. (2009)
Range: 0.001-0.007 ng m^{-2} min^{-1}	Station Nord, Greenland	Flux gradient method	Ferrari et al. (2004)
Range: 0-0.8 ng m^{-2} min^{-1}	Ny Ålesund, Svaldbard	Flux chamber	Ferrari et al. (2005)
Max: 0.58 ng m^{-2} min^{-1}	Ny Ålesund, Svalbard	Flux chamber	Ferrari et al. (2008)
Mean: 0.13 ng m^{-2} min^{-1}	Ny Ålesund, Svalbard	Flux chamber	Sommar et al. (2007)